

A novel closed-loop vacuum silicon microgyroscope

Xia Dunzhu Wang Shourong Zhou Bailing

(School of Instrument Science and Engineering, Southeast University, Nanjing 210096, China)

Abstract: A novel closed-loop control strategy of a silicon microgyroscope (SMG) is proposed. The SMG is sealed in metal can package in drive and sense modes and works under the air pressure of 10 Pa. Its quality factor reaches greater than 10 000. Self-oscillating and closed-loop methods based on electrostatic force feedback are adopted in both measure and control circuits. Both single side driving and sensing methods are used to simplify the drive circuit. These dual channel decomposition and reconstruction closed loops are applied in sense modes. The testing results demonstrate that useful signals and quadrature signals do not interact with each other because of the decoupling of their phases. Under the condition of a scale factor of $9.6 \text{ mV}/((^\circ) \cdot \text{s})$, in a full measurement range of $\pm 300 (^\circ)/\text{s}$, the zero bias stability reaches $28 (^\circ)/\text{h}$ with a nonlinear coefficient of 400×10^{-6} and a simulated bandwidth of more than 100 Hz. The overall performance is improved by two orders of magnitude in comparison to that at atmospheric pressure.

Key words: silicon micro-gyroscope (SMG); self oscillating; dual-channel closed-loop detection; scale factor; zero bias stability

The SMG is a kind of important inertial sensor. The inertial instruments attached to them are widely used in aerospace measurement, balance control, and vehicle navigation systems. At present, the gyroscope designed by many domestic institutes is only working in the atmospheric pressure environment. Obviously, it not only severely limits the sensor's sensitivity and system precision, but it also needs a more complicated matching circuit to detect an extraordinary weak varying capacitance signal (0.01 aF level)^[1-2]. Because open-loop detection can simplify the detection circuits, it is favorable for the integration and miniaturization of the measurement-control circuits, and it can meet the requirements of low-precision SMG specifications. Moreover, this method has been successfully applied in many foreign gyroscopes^[3-4]. However, in order to ensure a certain measurement bandwidth and no resonance peak during open-loop testing, it is essential that there should be a certain frequency difference between drive and sense modes. Meanwhile, it will inversely limit the quality factor of the detection mode and the whole mechanical sensitivity even if the bandwidth is acquired, and it probably also causes a relatively low SNR of the interface circuit. So gyroscopes with the above methods will have low precision. Furthermore, the open-loop detection is likely affected by the nonlinear characteristics be-

tween detection displacement and its corresponding capacitance, which makes it have a limited measurable angular range. Especially, the application circumstances of the gyroscope are complicated and it is usually affected by many kinds of disturbances such as outer interference, over shock, vibration and so on. The open-loop detection cannot ensure the stability and reliability of SMG's output. Therefore, in order to improve accuracy and reliability, a novel dual-channel closed-loop detection method is presented and successfully implemented in this paper.

1 Design Schemes of the SMG in Drive and Sense Modes

1.1 Self-oscillating scheme in drive mode

Currently most SMGs utilize capacitive electrostatic excitation^[5-6], which can guarantee that the driving frequency ω_d approaches the natural frequency ω_{nx} in the drive mode as closely as possible, and the amplitude is as stable as possible. To satisfy these requirements, the closed-loop control must be achieved in the actuation of the SMG. Nowadays, the closed-loop actuation of the SMG commonly adopts automatic gain control (AGC), which implements the closed-loop driving by means of a nonlinear control, thus reducing the closed-loop gain of the entire loop to one. This paper suggests an improved scheme of self-oscillation of the SMG, which achieves the closed-loop control utilizing a nonlinear relationship between DC voltage used for control and the driving force. The scheme succeeds in decoupling the phase angle and gain of the self-oscillation, where the angle and gain can be optimized and adjusted separately. It can increase the stability of the drive frequency and the amplitude. From the analyses above, the role of the closed-loop control of the driving circuit is to make relative deviation $|\Delta\omega/\omega_d|$ as small as possible and to increase the stability of the driving frequency and the amplitude.

As shown in Fig. 1, a whole scheme of the driving circuit method is realized by composition of SMG's transfer function in the drive mode, the K_{xc} module (the transfer coefficient from combo finger displacement to its equivalent capacitance), the K_{cv} module (the transfer coefficient from capacitor to voltage), the AGC loop, the phase shifter module, and the force feedback generator module. In the AGC loop, the PID controller module can ensure that the oscillating amplitude of the gyroscope in the drive mode is equal to the setting value by adjusting V_{ref} , and the absolute value circuit can complete the rectification of the demodulated AC signal.

1.2 Dual-channel closed-loop detection of SMG

The output signals of the SMG are complicated. They principally contain two parts, the quadrature signal and the Coriolis signal, which are orthogonal to each other^[7-8]. The

Received 2008-08-21.

Biography: Xia Dunzhu (1978—), male, doctor, lecturer, xiadz_1999@163.com.

Foundation items: The National High Technology Research and Development Program of China (863 Program) (No. 2002AA812038), the National Defense Pre-Research Support Program (No. 41308050109).

Citation: Xia Dunzhu, Wang Shourong, Zhou Bailing. A novel closed-loop vacuum silicon microgyroscope[J]. Journal of Southeast University (English Edition), 2009, 25(1): 63 – 67.

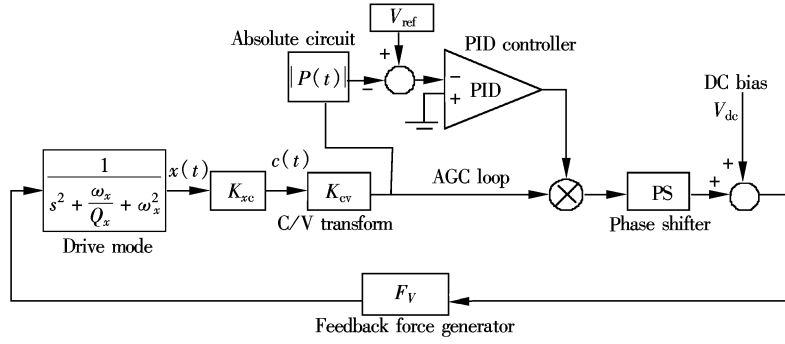


Fig. 1 Scheme of driving circuit method

quadrature signal contains the quadrature coupling signal and one part of the displacement coupling signal. The Coriolis channel contains the Coriolis signal and the other part of the displacement coupling signal. For the gyroscope with changing-distance detection, the displacement coupling signal is much weaker than the quadrature coupling signal so

that it is easy to separate the interfering signal from the Coriolis signal. According to the theory of signal processing, the only optimal way of separating the interfering signal from the Coriolis signal is phase modulation and demodulation. The dual-channel closed-loop detection block diagram of the kind of the SMG mentioned above is given in Fig. 2.

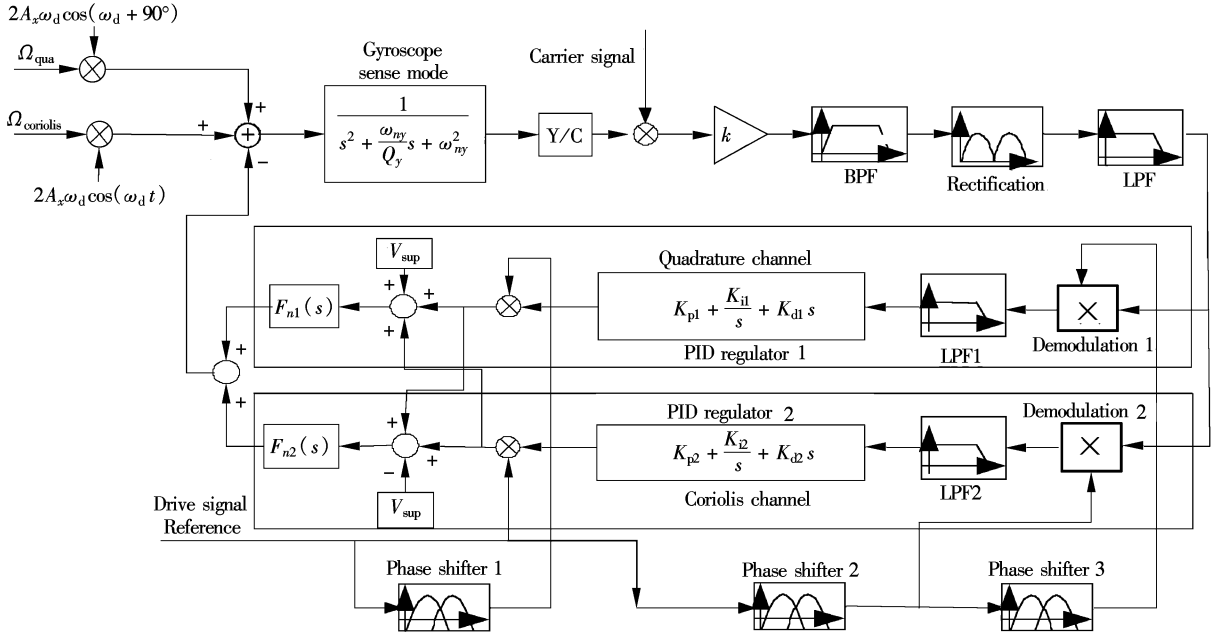


Fig. 2 The block diagram of dual-channel closed-loop control

As shown in Fig. 2, the Coriolis signal S_{cor} and the quadrature signal S_{qua} are expressed respectively as

$$S_{cor}(t) = 2A_x\omega_d\cos(\omega_d t)\Omega_{cor} \quad (1)$$

$$S_{qua}(t) = 2A_x\omega_d\cos(\omega_d t + 90^\circ)\Omega_{qua} \quad (2)$$

where A_x is the oscillation amplitude in the drive mode; ω_d is the driving frequency which is the same as its natural frequency ω_{nx} according to the designed structure parameters; Ω_{cor} and Ω_{qua} are the input angular rates of the Coriolis signal and the equivalent quadrature signal, respectively, and they are 90° out-of-phase. According to the superposition principle in control theory, both of them can be separately analyzed. The common forward part, including the transfer function of the gyroscope in the sense mode, the Y/C module (the conversion coefficient from displacement in the sense direction to variable capacitor), K (the total gain of amplifiers), the BPF (band-pass filter), the rectification

module (for the first demodulation of both two signals), and the LPF (low-pass filter) can pick off these two mixed signals. There are two channels including the quadrature channel and the Coriolis channel, which are both composed of the second demodulation module, LPF, PID regulator, and electrostatic force feedback generator $F_n(s)$, which can be adjusted by changing the preload voltage V_{sup} . Thus, the whole block diagram constructs the dual closed-loop detection of a gyroscope in the sense mode.

2 Simulation of System Bandwidth Calibration

According to the front block diagram of the dual-channel closed-loop control, Fig. 3 shows the simplified control scheme of closed-loop detection only in the Coriolis signal channel because the two channels have the same systematic framework. Through this control strategy, the final effect is that the quadrature part is completely suppressed and the output signal can automatically follow the input angular signal Ω_{cor} .

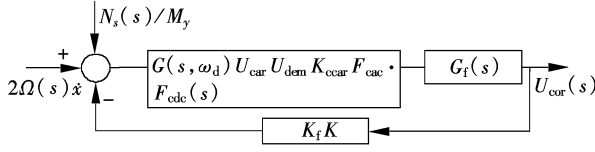


Fig. 3 The simplified block diagram of Coriolis signal closed-loop detection

As shown in Fig. 3, $2\Omega(s)\dot{x}$ is the Coriolis acceleration; $N_s(s)/M_y$ is equivalent to the input angular rate noise; $K_f K$ is the actuator and adjustable feedback gain; $G(s, \omega_d) U_{car} U_{dem} K_{ccar} F_{cac}(s) K_{cac} K_{cdc}(s)$ is the forward path transfer function; and $G_f(s)$ is a PID regulator model.

In fact, the principle of the dual-channel closed-loop detection achieved by the quadrature channel is the same as the one achieved by the Coriolis channel. Both the processed signals have the same frequency that is equal to the natural frequency in the SMG's drive mode; the differences between them are the phase angle and the changing trend. So the closed-loop detection with these two channels, essentially, is an AC feedback servo system. It should be controlled to maintain the balance of the AC force which means that there is an almost null displacement for proof mass in the sense direction. Considering a special AC force feedback, these two channels need both modulation and demodulation, which can achieve a quick closed-

loop servo control. This is different from traditional servo systems. These two channels are orthogonally decoupled and do not interfere with each other, so we can analyze the closed-loop control performance of the two channels, respectively. For the useful signal channel, the Coriolis channel, the closed-loop transfer function of the gyro is calculated as follows^[9]:

Let $G_0(s) = G(s, \omega_d) U_{car} U_{dem} K_{ccar} F_{cac}(s) K_{cac} K_{cdc}(s)$ and

$G(s, \omega_d) = \frac{K_{y-v}}{s^2} + \frac{\omega_{ny}}{Q_y s} + \omega_{ny}^2$, then

$$G_c(s) = \frac{G_0(s)}{1 + G_0(s) K_f G_f(s)} = \frac{\frac{K_{y-v} U_{car} U_{dem} K_{ccar} F_{cac}(s) K_{cac} K_{cdc}(s)}{s^2 + \omega_{ny}/Q_y s + \omega_{ny}^2} \left(K_p + \frac{K_p}{T_i} s + K_p \tau s \right)}{1 + \frac{K_{y-v} U_{car} U_{dem} K_{ccar} F_{cac}(s) K_{cac} K_{cdc}(s)}{s^2 + \omega_{ny}/Q_y s + \omega_{ny}^2} K_f \left(K_p + \frac{K_p}{T_i} s + K_p \tau s \right)} \quad (3)$$

where the PID regulator $G_f(s) = K_p + \frac{K_p}{T_i} s + K_p \tau s$.

Obviously, the closed-loop transfer function is a high-order system. It can be computed through Matlab tools. The effect of the PID regulator's parameters on the system bandwidth is shown in Tab. 1, and Fig. 4 shows the simulation results.

Tab. 1 Effect of the PID regulator's parameters on the system bandwidth

PID regulator's parameters	$\frac{0.002s^2 + 0.5s + 1}{s}$	$\frac{0.0015s^2 + 2s + 1}{s}$	$\frac{0.0025s^2 + 3s + 1}{s}$	$\frac{0.005s^2 + 3s + 2}{s}$
K_p	0.5	2	3	3
T_i/s	0.5	2	0.3	1.5
τ/ms	4	7.5	2.5	2.5
Simulated bandwidth/Hz	60	99.8	146	205

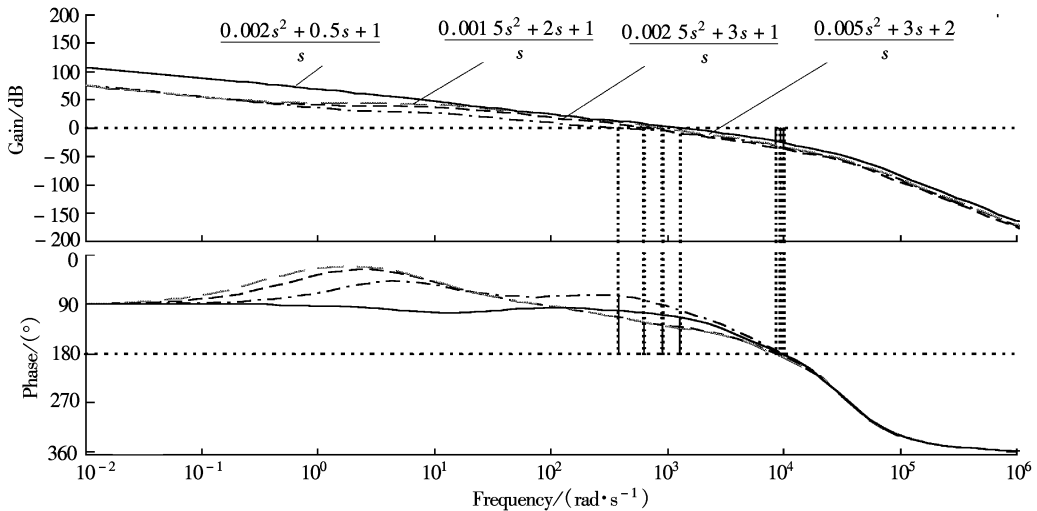


Fig. 4 The simulated Bode graph of the whole closed-loop system

It can be seen from Tab. 1 that changing the transfer function of the calibration module (just changing the PID parameters: the proportional coefficient K_p , time integral constant T_i , time differential constant τ) can influence the closed-loop system bandwidth of a gyroscope. Fig. 4 illustrates the changes of the closed-loop system bandwidth with different calibration models, and the system Bode graph

shows the changes in amplitude margin and phase margin. So when designing the calibration model, we should not only meet the system bandwidth requirements, but also consider the stability of the system. The closed-loop system shown in Fig. 4 is stable and reliable with the phase margin greater than 45° and the amplitude margin greater than 30 dB.

3 Experimental Results

An SMG with a structure of changing-distance capacitor detection is adopted in this paper. The SMG named as E17 is sealed in metal can package so that it works under an air pressure of 10 Pa with a quality factor of above 10 000. A miniature prototype scheme based on PCB technology has been realized with a volume size of 40 mm × 40 mm × 30 mm and a power consumption of less than 300 mW. The testing results at 25 °C demonstrate that the useful signal and the quadrature signal do not interact due to their phase decoupling. Under the condition of a scale factor of 9.6 mV/((°) · s), the zero bias stability reaches below 28(°)/h

with a nonlinear coefficient less than 400×10^{-6} and a simulated bandwidth more than 100 Hz. The overall performance is improved two orders of magnitude compared with that at atmospheric pressure. The engineering work is in progress at present.

A miniature prototype of the SMG based on PCB and its testing platform are shown in Fig. 5, and the performance index of E17 summarized in Tab. 2 is tested to resolve thermal design, power, and electromagnetic compatibility. The experimental results testify that the miniature prototype of the SMG can be realizable without changing its original performance. The testing results for scale factor and zero bias stability are shown in Fig. 6 and Fig. 7.

Tab. 2 Performance index of E17

Technical data		Value
Performance (25 °C)	Bias stability/((°) · h ⁻¹)	28
	Noise/((°) · s ⁻¹ · Hz ^{-$\frac{1}{2}$})	0.002 4
	Noise equivalent rate/((°) · s ⁻¹)	0.05
	Dynamic range/((°) · s ⁻¹)	± 300
	Sensitivity/((°) · s ⁻¹)	0.02
	Linearity	≤400 × 10 ⁻⁶
Power supply	Bandwidth/Hz	> 100
	Supply voltage/V	± 5
	Current dissipation/mA	30
Environment (- 40 to 80 °C)	Bias stability/((°) · s ⁻¹)	3
	Shock survival	1 000g
	Temperature drift/((°) · s ⁻¹ · °C ⁻¹)	< 0.03

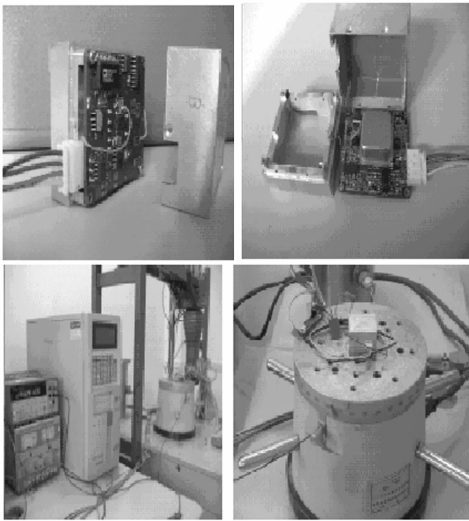


Fig. 5 The graph and testing platform of miniature prototype microgyro

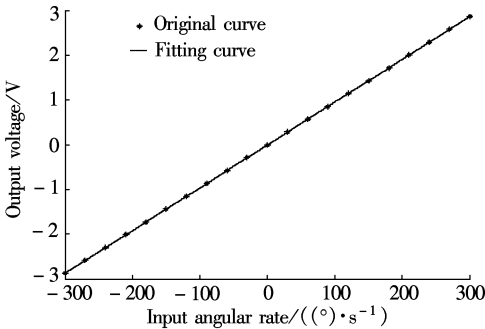


Fig. 6 Scale factor testing

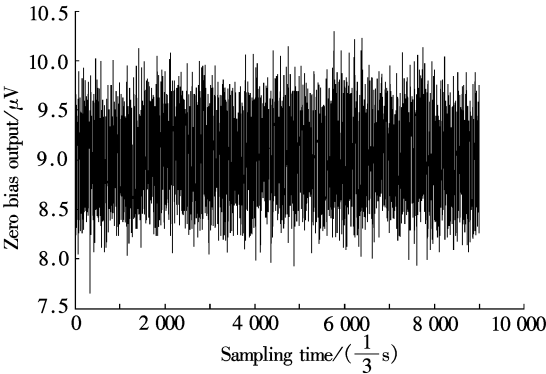


Fig. 7 Zero bias stability testing

4 Conclusion

The application circumstances of the gyroscope are complicated, usually affected by many kinds of disturbances such as interference, over shock, vibration and so on. In addition, the bandwidth of an SMG is approximately determined by the designed frequency difference between drive and sense modes. In order to improve the accuracy and reliability and broaden the system bandwidth, a novel dual-channel closed-loop detection method is adopted in this paper, which ensures the stability and reliability of the silicon

micro-gyroscope’s output by testing some kinds of performance of an SMG. Finally a miniature prototype of an SMG based on PCB is successfully designed, and the performance list is tested to resolve thermal design, power, and electromagnetic compatibility. The experimental results testify that

the miniature prototype of an SMG is realizable without changing its performance. Nevertheless, some important performances such as the temperature characteristics of an SMG's zero bias output and scale factor will be perfected through further efforts^[10-11].

References

- [1] Tang T K. A packaged silicon MEMS vibratory gyroscope for microspacecraft [C]//*Proc IEEE MicroElectro Mechanical Systems*. Nagoya, 1997: 500 – 505.
- [2] Sharma A, Zaman M F, Ayazi F. A 0.2/hr micro-gyroscope with automatic CMOS mode matching [C]//*Proc IEEE Int Solid-State Circuits Conf Dig Tech Papers*. San Francisco, CA, 2007: 386 – 387.
- [3] Saukoski M, Aaltonen L, Salo T, et al. Integrated readout and control electronics for a microelectromechanical angular velocity sensor [C]//*Proc Eur Solid-State Circuits Conf*. Montreux, Switzerland, 2006: 243 – 246.
- [4] Phani A S, Seshia A A, Palaniapan M, et al. Modal coupling in micromechanical vibratory rate gyroscopes[J]. *IEEE Sensors Journal*, 2006, 6(5): 1144 – 1152.
- [5] Loveday P W, Rogers C A. The influence of control system design on the performance of vibratory gyroscopes[J]. *Journal of Sound and Vibration*, 2002, 255(3): 417 – 432.
- [6] Tang William Chi-Keung. Electrostatic comb drive for resonant and actuator applications[D]. Berkeley: University of California at Berkeley, 1990.
- [7] Yeh Bao Y, Liang Yung C. Mathematical modelling on the quadrature error of low-rate microgyroscope for aerospace applications [J]. *Analog Integrated Circuits and Signal Processing*, 2001, 29(1/2): 85 – 94.
- [8] Saukoski Mikko, Aaltonen Lasse, Halonen Kari A I. Zero-rate output and quadrature compensation in vibratory MEMS gyroscopes[J]. *IEEE Sensors Journal*, 2007, 7(12): 1639 – 1652.
- [9] Zeng Hui, Zhou Bailing, Su Yan, et al. Research of MEMS gyroscope detection feedback control system [J]. *Sensor Technology*, 2005, 25(6): 32 – 34. (in Chinese)
- [10] Ferguson Michael I, Keymenlen Didier, Peay Chris, et al. Effect of temperature on MEMS vibratory rate gyroscope [C]//2005 *IEEE Aerospace Conference Proceedings*. Big Sky, MT, USA, 2005: 1 – 6.
- [11] Shcheglov K, Evans C, Gutierrez R, et al. Temperature dependent characteristics of the JPL silicon MEMS gyroscope [C]//2000 *IEEE Aerospace Conference Proceedings*. Big Sky, MT, USA, 2000: 403 – 411.

一种新型的闭环真空硅微陀螺仪

夏敦柱 王寿荣 周百令

(东南大学仪器科学与工程学院, 南京 210096)

摘要:提出了一种新型的硅微陀螺仪闭环控制策略. 所设计的硅微陀螺仪工作在 10 Pa, 采用金属壳 CAN 封装形式, 驱动和检测两模态品质因素高达 10 000 以上, 且都采用了基于静电力反馈方法实现闭环. 驱动模态采用单边驱动单边检测, 尽量使线路简化; 检测模态采用双重分解和重构闭环回路. 测试结果表明: 有用信号和正交信号实现很好的相位解耦, 互不影响; 在满量程 ± 300 ($^{\circ}$)/s、标度因素 $9.6 \text{ mV}/((^{\circ}) \cdot \text{s})$ 的情况下, 零偏稳定性已达到 28 ($^{\circ}$)/h; 非线性度达到 400×10^{-6} ; 仿真带宽大于 100 Hz. 这较以前设计的仅在空气下工作的硅微陀螺性能提高了近 2 个数量级.

关键词: 硅微陀螺仪; 自激振荡; 双闭环检测; 标度因素; 零偏稳定性

中图分类号: U666. 112